DOI: https://doi.org/10.15407/pmach2021.02.037

UDC 539.4:621.165

INVESTIGATION OF THE THERMAL STRENGTH OF STEAM TURBINE DIAPHRAGMS WITH REDUCTION OF AXIAL DIMENSIONS

[1] Borys P. Zaitsev
b.zajtsev@gmail.com
ORCID: 0000-0003-2411-0370

[2] Viktor L. Shvetsov
shvetsov@turboatom.com.ua
ORCID: 0000-0002-2384-1780

[2] Oleksandr M. Hubskyi

[2] Serhii A. Palkov
sergpalkov@gmail.com
ORCID: 0000-0002-2215-0689

[1] Tetiana V. Protasova
tatyprotasova@gmail.com
ORCID: 0000-0003-1489-2081

[1] A. Pidhornyi Institute of Mechanical Engineering Problems of NASU
2/10, Pozharskyi St., Kharkiv, 61046, Ukraine

[2] Joint-Stock Company Turboatom
199, Moskovskyi Ave., Kharkiv, 61037, Ukraine

The problem of reducing the axial dimensions of steam turbine diaphragms is associated with the problem of steam turbine modernization performed by increasing the number of reactive blading stages and using existing foundations. Evaluation of the suitability of diaphragm design versions with established steam flow characteristics was carried out with constraints on short- and long-term strength conditions, as well as the accumulation of axial deflections due to creep. For computational research, there was introduced a methodology using the finite element method and Yu. M. Rabotnov's theory of strain aging. The calculation of creep was reduced to solving an elastic-plastic problem with a deformation curve, which was represented by an isochronous creep curve for the time chosen. A software was used providing for the automated construction of the original computer diaphragm model with the help of guide-vane profile drawings and axial cross-sections of the diaphragm rim and body, as well as several geometric parameters. The calculated model of a welded diaphragm reproduces the main essential features of the structure, the material properties of its elements, as well as steam load. The exploratory studies of diaphragms with reduced axial dimensions were performed on the example of the second- and third-stage diaphragms of the high-pressure cylinder of the K-325-23.5 steam turbine. The original second- and third-stage diaphragm designs were considered to be basic, in relation to which, according to strength and rigidity parameters, the alternative ones were compared. Calculated data for the basic diaphragm design versions for 100 thousand operating hours were obtained. According to the calculations, maximum deflections are achieved at diaphragm edges, and the stresses, that are maximum at the points where the guide vanes are attached to the diaphragm rim and body, undergo a significant redistribution due to creep. Two approaches to the reduction of the axial dimensions of the second-stage diaphragm design of the steam turbine high pressure cylinder were involved. In the first approach, the reduction of the dimensions was achieved by proportionally reducing the guide-vane profile with a corresponding increase in the number of the guide vanes. In the second approach, the profile remained unchanged, but the axial dimensions of the diaphragm rim and body were reduced. The parameters of strength both in the elastic state at the beginning of operation and in the conditions of creep, as well as the accumulation of axial deflections were investigated. Based on the comparisons with the basic design, it was established that the second approach is more effective. Additional recommendations for the use of more heat-resistant steels for outlet guide vanes and the conditions of diaphragm attachment in the turbine casing are given.

Keywords: *steam turbine, diaphragm, axial dimensions, creep, axial deflection, short- and long-term strength.*

Introduction

One of the aspects of deep turbine modernization is to increase the number of stages, in particular in the high-pressure cylinder (HPC), and the use of reactive blading, which can significantly increase efficiency. Steam turbine modernization is performed using the existing foundation, which necessitates the reduction of the axial dimensions of the stages. The simplest way is to reduce the axial dimensions due to the greater compactness of steam turbine diaphragms. However, it is necessary to ensure the basic indicators of long-term rigidity and strength of the diaphragms. Because of this, there arises the problem to assess the possibility of structural changes in the most loaded diaphragms of a steam turbine HPC according to the criteria of strength in high temperature conditions, which is considered on the example of the K-325-23.5 steam turbine.

The main issues of ensuring the reliable operation of the diaphragms are to assess the short- and long-term strength of their elements; determine the rate of increase of the deflections due to material creep (for stages with a steam temperature above 450 °C); ensure sufficient diaphragm tightness over the entire support surface.

Theoretical and experimental solutions of these problems are reflected in [1–4], which propose models and methods for calculating diaphragms in elastic formulation. The contact interactions of diaphragm support elements with the turbine casing, which affect the stress-strain state (SSS) and contact tightness, are considered in [5–7], and the state of the diaphragms during creep, in [8–10].

In most works, plate-rod models are used, in which the diaphragm rim and body are modeled using semicircular plates, and the guide-vane assembly is modeled using a regular system of rods that undergo unsymmetrical bending. These models reflect the main features of diaphragm deformation, but do not allow us to consider the influence of a number of important design factors, which necessitates the use of three-dimensional models. In this, it is important to:

– model the SSS of guide vanes for intermediate- and high-pressure cylinder diaphragms, which are not rod bodies;

– model guide-vane attachment to the rim and body, especially complex for welded diaphragms;

– represent the real features of the protrusion of the outlet guide vanes beyond the joint face, where the stress level is much higher than that in the middle guide vanes of the assembly;

– take into account the pliability of the diaphragm support contour;

– take into account the deformation of creep, which affects the accumulation of axial diaphragm deflections and stresses in the welds of diaphragm guide vanes to determine their durability.

When designing diaphragms, for simplicity, it is assumed that the main mode of steam turbine diaphragm operation is the stationary one with a constant temperature field and system of loads due to steam flow. Under such assumptions, the approach to creep calculations is simplified, which makes it possible to apply much simpler theories of strain aging [11]. The application of a theory of aging is justified by the fact that the creep of steam turbine diaphragms occurs mainly in stationary modes [1], which are characterized by a steady state of creep, where calculations are traditionally performed using isochronous curves [12].

In reality, the operation of steam turbine diaphragms is accompanied by a significant number of partial or complete load drops, which is especially true for switching modes. In this case, the load on a diaphragm is variable, which puts forward increased requirements for the methodology of creep calculations, and necessitates the use of incremental creep theories capable of tracking the entire process of loading [13].

In a number of works, three-dimensional modeling in diaphragm calculations was performed by the super-element method [14] in the elastic region of deformation and by the multi-grid method in the elastic region [7], as well as in the state of creep [13, 15].

Thus, these problems of ensuring the reliable operation of the welded diaphragms of steam turbines can be solved on the basis of three-dimensional modeling of elastic deformation and creep state, using the finite element method (FEM), and constructing an effective mathematical support for the SSS parameters that determine short- and long-term strengths.

A Method for Calculating Welded Diaphragms in Elastic Deformation and with Account of Creep

In designing diaphragms, short-term strength must be ensured, i.e. strength at every instant of turbine operating time. This requires limiting maximum stresses, especially at the beginning of turbine operation, when the diaphragms are still in the elastic deformation region, and creep processes have not yet developed. It is in the elastic region that stress deformations in the diaphragms acquire maximum values, and therefore the assessment of short-term strength is performed according to the calculations for the elastic state. Fulfillment of the conditions of long-term operation is associated with the study of creep processes that develop over time, causing the accumulation of axial deflections, stress redistribution, and accumulation of damage, which is the reason for the long-term strength constraint.

The methodology for calculating the strength of the welded diaphragms of steam turbines is based on the use of FEM, which is applied to solve problems of elasticity and creep theories in three-dimensional formulation. An isoparametric finite element is used, whose ratios for displacements and Cartesian coordinates are the same

$$u_x = \sum u_{xi} N_i(\xi,\eta,\zeta), \quad u_y = \sum u_{yi} N_i(\xi,\eta,\zeta), \quad u_z = \sum u_{zi} N_i(\xi,\eta,\zeta); \tag{1}$$

$$x = \sum x_i N_i(\xi, \eta, \varsigma), \quad y = \sum y_i N_i(\xi, \eta, \varsigma), \quad z = \sum z_i N_i(\xi, \eta, \varsigma), \tag{2}$$

where $N_i(\xi, \eta, \zeta)$ are shape functions; ξ, η, ζ are local coordinates in the finite element; u_{xi}, u_{yi}, u_{zi} , and x_i, y_i, z_i are, respectively, the nodal values of the components of the displacement vector and the Cartesian coordinates of the nodes of the finite element.

The thermoelastic problem is formulated in variational statement using the principle of minimum total potential energy of a system for an orthotropic inhomogeneous body with the functional

$$\Phi = 0{,}5\int_V \hat{D}\hat{\varepsilon}\cdot\cdot\hat{\varepsilon}dV - \int_V \overline{F}_V\overline{u}dV - \int_{S_F} \overline{F}_S\overline{u}dS - \int_V \alpha T\hat{D}\hat{E}\cdot\cdot\hat{\varepsilon}dV\,, \tag{3}$$

where $\hat{D}$ is the tensor of elastic constants in an inhomogeneous orthotropic medium; $\overline{u}$ is the displacement vector; $\hat{\varepsilon}$ is the strain tensor; $\hat{E}$ is the unit tensor; $\overline{F}_V, \overline{F}_S$ are volume and surface forces; S_F is part of the surface where the forces $\overline{F}_S$ act; α is the thermal expansion coefficient.

The last term in expression (3), which corresponds to the temperature load, can be represented as follows:

$$-\int_V \frac{\alpha E}{1-2\nu}\theta T dV\,, \tag{4}$$

where E is the modulus of longitudinal elasticity; ν is Poisson's ratio; $\theta = \varepsilon_x + \varepsilon_y + \varepsilon_z$ is the volumetric strain.

Based on (4), on the basis of relations (1), (2), a general expression for the nodal values of the temperature load F_T on the finite element is obtained. In this, for simplicity, it is assumed that the characteristics of the material are constant

$$F_T = -\frac{\alpha E}{1-2\nu}\int_{CE} T(x, y, z)\sum_i \left(u_{xi}\frac{\partial N_i}{\partial x} + u_{yi}\frac{\partial N_i}{\partial y} + u_{zi}\frac{\partial N_i}{\partial z}\right)dV\,. \tag{5}$$

The $\partial N_i/\partial x$, $\partial N_i/\partial y$, $\partial N_i/\partial z$ values that enter into expression (5) are determined in Gaussian integration nodes. This uses the connection of Cartesian and local coordinates (2) to obtain at each point of the finite element (Gaussian nodes) of the Jacobian matrix elements ($\partial\xi/\partial x$, $\partial\xi/\partial y$, $\partial\xi/\partial z$, $\partial\eta/\partial x$, $\partial\eta/\partial y$, $\partial\eta/\partial z$, $\partial\zeta/\partial x$, $\partial\zeta/\partial y$, $\partial\zeta/\partial z$) of transformation of the coordinates $\xi(x, y, z)$, $\eta(x, y, z)$, $\zeta(x, y, z)$, invertible to (2). The full vector of the temperature load is obtained by summing up all finite elements.

The application of the FEM procedure in minimization (3) leads to a finite-element model of the problem of determining the SSS in the formulation of the three-dimensional theory of elasticity, presented by a system of high-order linear algebraic equations

$$Ku = f\,, \tag{6}$$

where K is the stiffness matrix; u is the displacement vector; f is the right hand-side vector.

System (6) usually has a banded structure, and its solution is performed through triangulating the stiffness matrix K, in particular by the method of square roots.

When solving the problem of creep, the theory of creep aging is involved, which well enough reflects the development of creep deformations at constant or slightly variable loads and temperatures. To maintain an acceptable solution time, the simplest Yu. M. Rabotnov's theory of creep aging [11] was used, which is based on the involvement of physical relations of the theory of small elastic-plastic deformations. To determine the SSS, the elastic-plastic problem is solved using isochronous creep curves, which are taken as a deformation curve. The solution of the elastic-plastic problem is carried out by the method of variable elasticity parameters [11] in the linearized material state relations

$$\varepsilon_{ii} = \frac{1}{E^*}\left[\sigma_{ii} - \mu^*(3\sigma_0 - \sigma_{ii})\right], \quad \varepsilon_{ij} = \frac{\sigma_{ij}}{G^*}\,, \tag{8}$$

where the variable elastic parameters are determined by the formulas

$$E^* = \frac{\frac{\sigma_i}{\varepsilon_i}}{1-\frac{1-2\mu}{3E}\cdot\frac{\sigma_i}{\varepsilon_i}}; \quad G^* = \frac{\sigma_i}{3\varepsilon_i}; \quad \mu^* = \frac{\frac{1}{2}-\frac{1-2\mu}{3E}\cdot\frac{\sigma_i}{\varepsilon_i}}{1-\frac{1-2\mu}{3E}\cdot\frac{\sigma_i}{\varepsilon_i}}. \tag{9}$$

The application of the method of variable elastic parameters is reduced to the iterations, in which the elastic problem with elastic variable-volume body parameters is solved, the parameters being determined either from the solutions of the problem in the previous iteration or with the elastic constants of the material (in a first iteration). The elastic parameters at the current iteration are calculated by the secant modulus σ_i / ε_i, using the deformation curve $\sigma_i(\varepsilon_i)$. The convergence of the iterative process is controlled by achieving a given accuracy according to the value of deformation.

Construction of a Computational Model for Determining the SSS Parameters a Diaphragm

There are various technologies to manufacture steam turbine diaphragms, but preference has recently been given to welded diaphragms. In such diaphragms the guide vanes are attached, using force welds, to the diaphragm body and rim and not to all blade end faces, i.e. there is an incomplete fusion zone a structural source of stress concentration. The basic idea of geometrical features of a welded diaphragm design is given in figures 1, 2 showing a general view of the half of the diaphragm, which is an independent load-carrying unit, and its schematic axial section with elements that are essential for modeling the SSS.

The construction of the calculation model is based on the analysis of the geometric design features, loading conditions, and interaction of the connectable turbine elements, and is briefly reduced to the following.

A steam turbine diaphragm has a horizontal joint that divides it into two keyed halves. It is assumed that there are no significant forces in the joint, and the two halves of the diaphragm are deformed independently, so only its half with the load-free surfaces of the joint is considered. The finite element model of the diaphragm is depicted in figure 3, which shows essential elements for modeling the SSS.

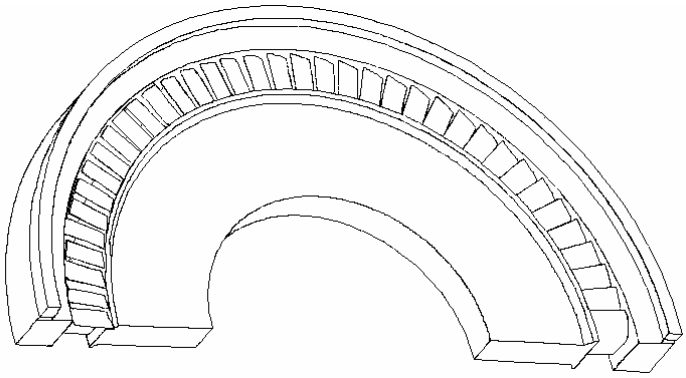

Fig. 1. Structural diagram of a steam turbine diaphragm

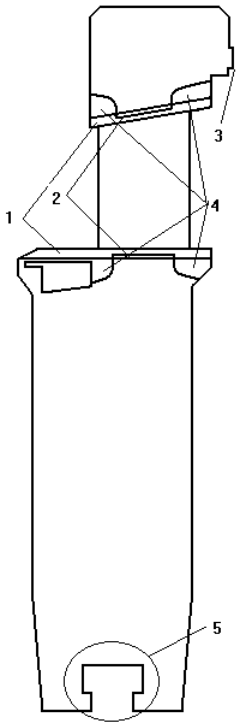

Fig. 2. Diaphragm cross-sectional scheme:
1 – shroud bands; 2 – technological hole under the guide vanes;
3 – protrusion for the axial support of the diaphragm; 4 – welding areas;
5 – area of attachment of the diaphragm labyrinth seal to the turbine shaft

The geometric model takes into account the guide-vane assembly, features of the welded connection of the guide vanes with the diaphragm body and rim with the representation of incomplete structural fusion, features of the protrusion of one of the outlet guide vanes beyond the joint face (joint face II in figure 3), diaphragm support elements (tooth and support lug)).

The external load on the diaphragm elements is due to steam pressure, the parameters of which at the diaphragm inlet and outlet are known. Therefore, the pressure distribution on the working part of the surface was assumed to be uniform with the transfer of the total force corresponding to the pressure drop and the ring area occupied by the guide-vane assembly. A load equal to the pressure drop was applied to the diaphragm rim and body from the side of the inlet stream, and a system of forces simulating the transmission of forces from the shaft sealing segments, which are also exposed to steam pressure, was applied to the diaphragm body across the end face of the axial groove under the shaft.

The resultant force from the gasdynamic forces on the guide-vane assembly has both axial and circumferential components. The axial component of all the loads on the diaphragm is carried by the support lug made in the turbine casing, and the circumferential component is carried by the keys located between the diaphragm and casing. The fastening of the diaphragm in the turbine casing was modeled by pinching the tooth on the outer cylindrical surface and discrete fixing of the rim in the circumferential direction on three sections of the outer surface near the joint and in the middle of the rim.

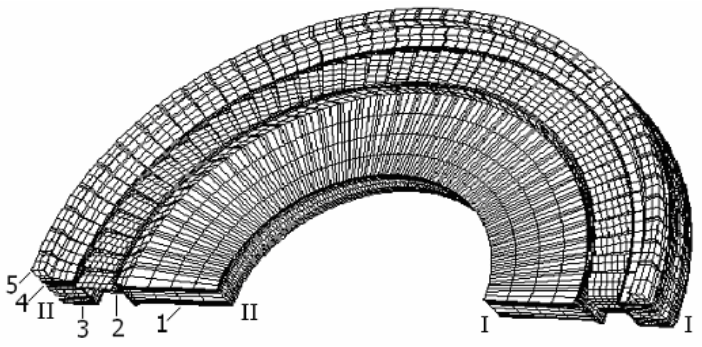

Fig. 3. Finite element model of the diaphragm:
1 – body; 2 – guide vanes; 3 – rim; 4 – support lug; 5 – body tooth; I, II – joint faces

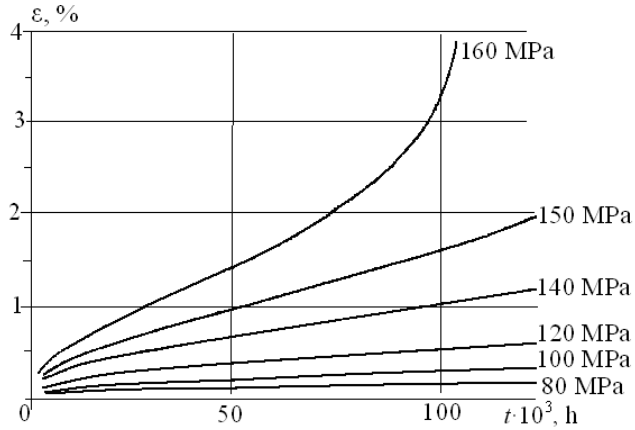

Fig. 4. Creep curves of the diaphragm material

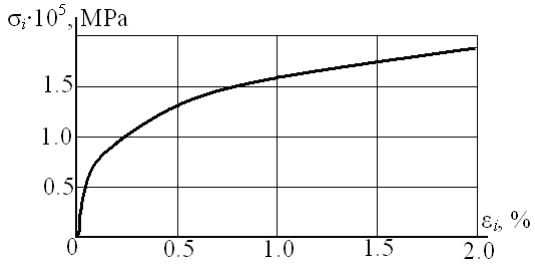

Fig. 5. Isochronous curve for the 15H11MF steel at a temperature of 503 °C for 10^5 operating hours

Thus, the given calculation model takes into account all the main features of the design and load of the diaphragm.

The original properties of the material during creep are represented by the creep curves (Fig. 4) of the materials of the guide vanes (steel 15H11MF), as well as diaphragm body and rim (steel 15H1M1F).

Data from the isochronous curves for the main material of the guide vanes, diaphragm body and rim, as well as of the welds (Fig. 5) were obtained on the basis of the creep curves of the diaphragm material.

The isochronous curves of the 15H11MF steel at a temperature of 503ºC for 10^5 operating hours were defined according to the dependence

$$\varepsilon = \frac{\sigma}{E} + 10^{-2}\left(\frac{\sigma}{\sigma_{1/10^5}}\right)^m,$$

where m=4; E=1.77 10^5 MPa; $\sigma_{1/10^5}$=160 MPa.

It is difficult to predict the weld material properties, which depend on many factors: the material of the electrodes to be used, the quality and uniformity of welding, the degree of additive burnout, etc. [16–17]. For the weld material, the creep resistance can be significantly reduced, which changes the shape of the isochronous curves. An example of research taking into account the influence of welds on diaphragm creep is the work [15]. In our research, the mechanical properties of the materials of the guide vanes, diaphragm rim and body, and welds were assumed to be identical.

The software package [15] involved in the computational research has advanced input and output interfaces, as well as a parametric scheme for constructing computational models, which greatly simplifies data preparation, increasing the reliability of their formation. In building the computational computer model of a diaphragm, the original data are the diagrams of the guide vanes and the axial cross-section of the diaphragm, which can be depicted by background drawings, numerical data on the number of the guide vanes, geometric parameters for the location of the guide vane assembly along the axis, outlet guide-vane protrusion beyond the joint face, radial seals, as well as data on elastic characteristics and creep.

Research of the Short- and Long-term Strengths of the Basic Design Version of K-325-23.5 Turbine HPC Diaphragms

The most stressed, especially in terms of long-term strength, are the second- and third-stage HPC diaphragms. Since this paper aims to change the design of the diaphragms with a decrease in axial dimensions while maintaining strength, it is necessary to have the estimated data on the SSS of the original designs of these diaphragms. It is in relation to the parameters of the short- and long-term strengths of the original diaphragm designs, as well as to the data on the yield and long-term strength limits [18] that the suitability of the proposed diaphragm design is determined.

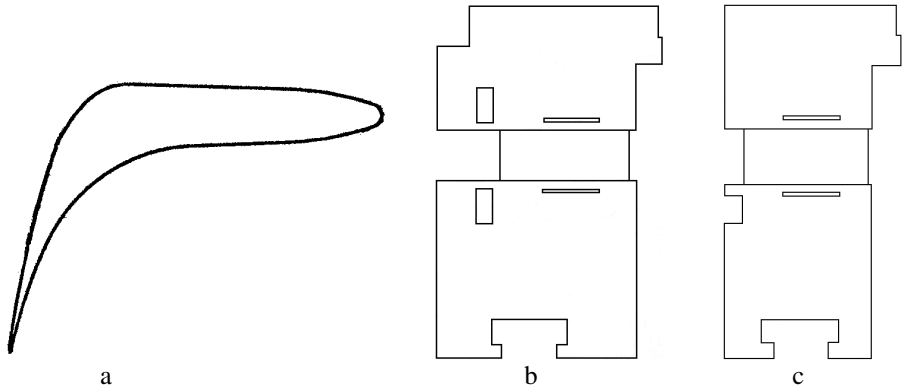

Fig. 6. Geometric data for modeling the second- and third-stage HPC diaphragms of the K-325-23.5 turbine:
a – guide vane profile (second and third stages); b – axial cross-section (rim and body) of the second-stage diaphragm; c – axial cross-section (rim and body) of the third-stage diaphragm

Table 1. Data on the design, material and operating conditions of the second- and third-stage HPC diaphragms

Indicator	Second stage	Third stage
Temperature before the stage, ºC	506	483
Number of guide vanes (half of the diaphragm)	29	29
Elastic modulus, GPa	177.6	182.2
Minimum diaphragm radius, cm	30.5	30.5
Maximum diaphragm radius, cm	52.5	52.9
Diaphragm thickness, cm	14	11.2
Pressure drop, MPa	2.491	2.135
Seal height, cm	1.5	1.5
Guide-vane profile width (along the axis)	8.0092	8.0092
Guide-vane profile height (along the circumference), cm	5.7080	5.7079
Outlet guide-vane protrusion beyond the joint face, cm	1.71	1.72
Guide-vane material	15H11MF	15H11MF
Rim and body	15H1M1F	15H1M1F

Fig. 6 shows a common, for the two diaphragms, guide-vane profile and the axial cross-sections of the diaphragm rim and body. Numerical data on the design, material, and load conditions are summarized in Table 1.

In the calculations of the diaphragms of steam turbines operating at high temperatures, the maximum stresses in the elastic stage of deformation are limited, and must not exceed the yield strength at a given temperature with the required margin (according to OST 108961.02-79 the yield strength for the 15H1M1F steel at a temperature of 500 ºC is 210 MPa, and at that of 475 ºC, 220 MPa). In addition, there are requirements for the accumulation of creep-induced axial deflections, which can reduce the required gaps, and the maximum stresses that determine the long-term strength.

Based on this, in the researches, the diaphragm SSS calculations were performed in the elastic region of deformation and creep for a period of 100 thousand operating hours. Detailed data from the calculations of the second-stage HPC diaphragm design are given in figures 7–9. In constructing the calculation model, two versions of modeling the guide-vane assembly were considered, related to the account of guide-vane shroud bands. In the first version, the shroud bands were considered to be load-carrying elements, and were attached to the diaphragm rim and body, the guide-vane length being shorter. In the second version, the shroud bands were not taken into account, and, accordingly, the guide-van length was longer. The calculation results in these cases differed slightly. In particular, in the elastic region of deformation, the maximum displacements in the first case were 0.443 mm, in the second one, 0.503 mm, i.e. the effect on the displacements is significant.

In the diaphragm with short guide vanes, the effect of creep on the strain state is insignificant, while the stress state undergoes significant changes. The maximum stresses are reduced (relaxation), and the load from the more stressed outlet guide vanes is transferred to the middle of the guide-vane assembly.

The strains and stresses in the third-stage diaphragm are generally similar, but their level is lower than in the second-stage diaphragm. Tables 2 and 3 show the maximum values of SSS parameters, which were determined from the whole structure, namely the deflections W along the diaphragm axis, the radial stress σ_r (along the guide vanes), and the circumferential stress σ_θ.

When modeling the attachment of the guide vanes to the diaphragm rim and body, the rigidity of the guide-vane shroud bands was taken into account, and the guide-vane profile discretization in thickness was two finite elements.

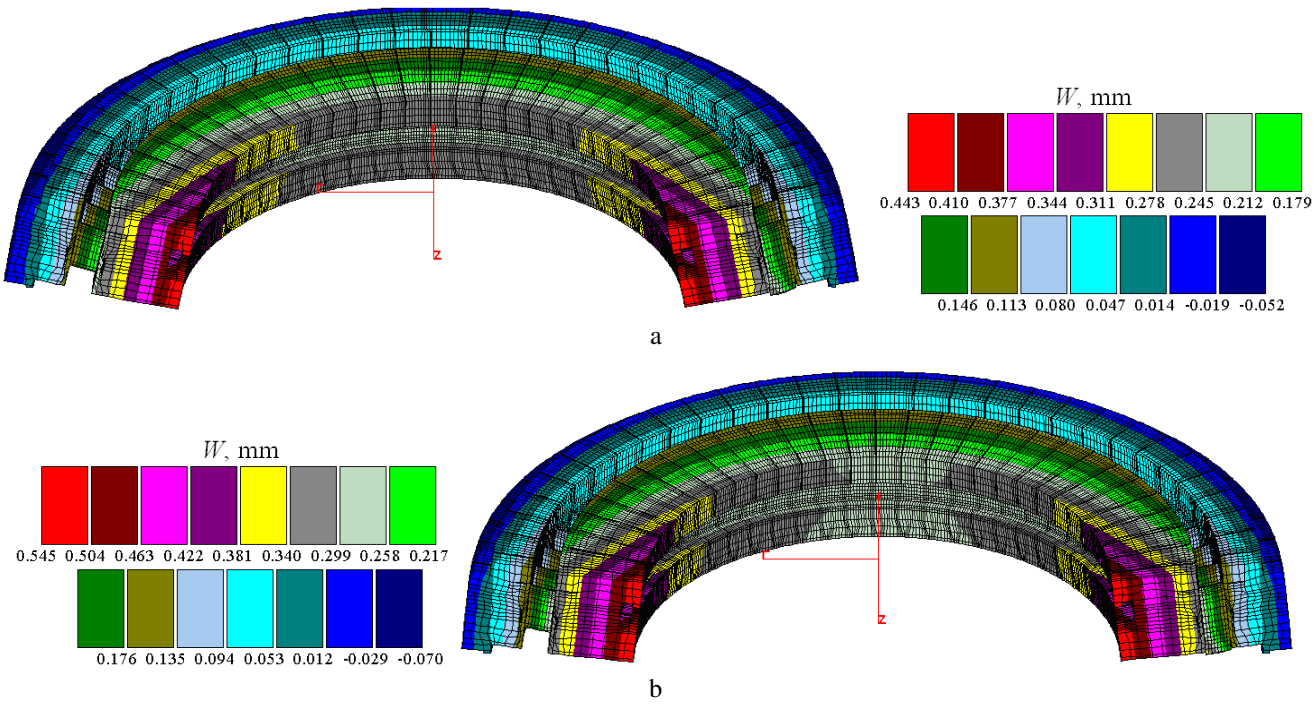

Fig. 7. Axial displacements in the diaphragm:
a – in the elastic state; b – during creep

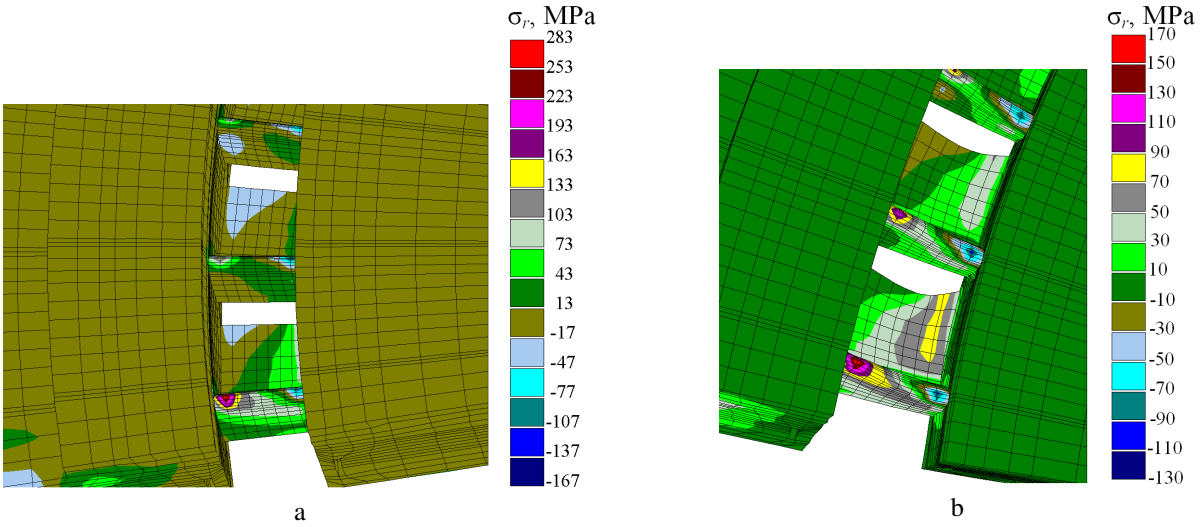

Fig. 8. Radial (along the guide vanes) stresses in the diaphragm guide vanes near the joint face:
a – in the elastic state; b – during creep

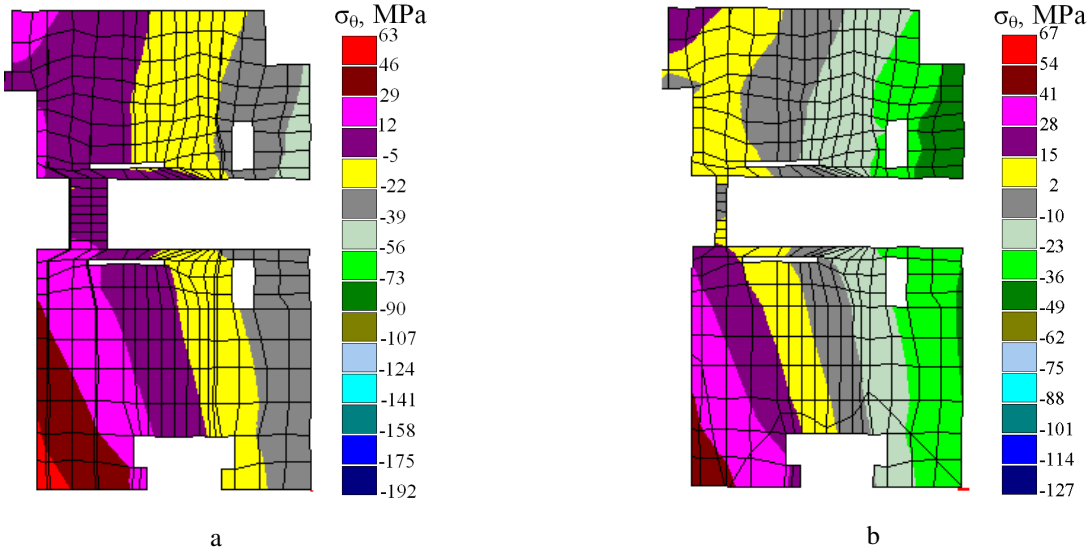

Fig. 9. Circumferential stresses in the rim and body in the middle cross-section of the diaphragm:
a – in the elastic state; b – during creep

Table 2. The maximum values of the SSS parameters of the second-stage diaphragm of the K-325-23.5 steam turbine HPC in the elastic state and during creep (100 thousand hours)

State	SSS parameter							
	Deflection W, mm		Radial stress σ_r, MPa				Circumstantial stress σ_θ, MPa	
	Seal	Blade root	Leading edge – body	Leading edge – rim	Trailing edge – body	Trailing edge – rim	Body	Rim
Elasticity	0.443	0.240	-90	268	148	118	54	-46
Creep	0.545	0.280	-104	161	120	80	48	-43

Table 3. The maximum values of the SSS parameters of the third-stage diaphragm of the K-325-23.5 steam turbine HPC in the elastic state and during creep (100 thousand hours)

State	SSS parameter							
	Deflection W, mm		Radial stress σ_r, MPa				Circumstantial stress σ_θ, MPa	
	Seal	Blade root	Leading edge – body	Leading edge – rim	Trailing edge – body	Trailing edge – rim	Body	Rim
Elasticity	0.610	0.310	-68	187	187	102	78	-64
Creep	0.762	0.380	-93	126	109	92	63	-50

Exploratory Researches of the Design Variants of the Second-stage HPC Diaphragm with Reduced Axial Dimensions

The main requirement for varying the design of the diaphragm to reduce its axial dimensions is the preservation of gas-dynamic indicators of the stage, which can be achieved in different ways. This paper proposes two approaches to changing diaphragm designs. In the first approach, transformations of the guide-vane assembly are introduced, which causes a proportional reduction in the size of the guide-vane profile in all directions (reduction coefficient k). To maintain the gas-dynamic indicators of the stage, the number of the guide vanes in the assembly is increased accordingly. The reduction of axial dimensions is achieved only by changing the guide-vane profile. In the second approach, the guide-vane assembly remains unchanged, while the thicknesses of the body and rim are reduced. Geometric data from the diaphragm designs for the considered options are given in figure 10 and in Table 4.

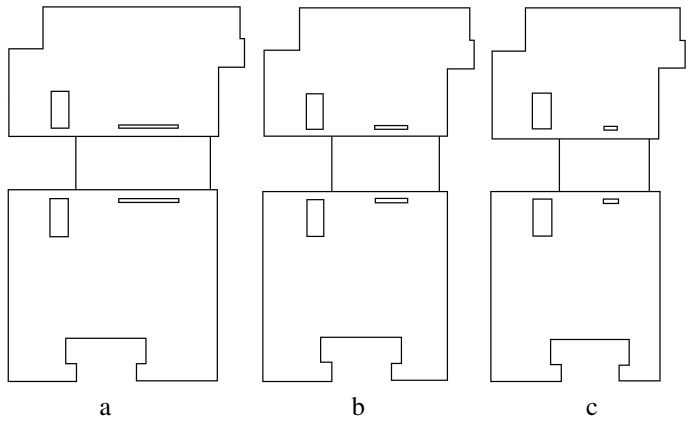

Fig. 10. Axial cross-sections of second-stage HPC diaphragms with reduced axial dimensions:
a – an original diaphragm; b – reduction by 1.55 cm (k=1.24); c – reduction by 2.60 cm (k=1,48)

Table 4. Parameters of the design models of the second-stage diaphragm of the K-325-23.5 steam turbine HPC

Version	Reduction coefficient of the guide-vane profile k	Number of guide vanes	Changes in the rim and body
1	1.00	29	Original
2	1.24	36	Axial reduction by 1.55 cm
3	1.48	43	Axial reduction by 2.60 cm
4	1.00	29	Axial reduction by 3.5 cm

Data on the maximum values of the SSS parameters of the diaphragm, obtained in the calculations, for all the versions of design changes are given in Tables 5–7. It should be noted that as the guide-vane profile decreases, the axial deflections, i.e. the diaphragm stiffness, significantly and rapidly increase with increasing parameter k. This also applies to the maximum stresses that develop, especially at the leading edge of the outlet guide vane near the diaphragm rim. Stresses are significantly higher than permissible according to [18], both in the elastic stage of deformation and in the phase of steady creep. This behavior follows from the fact that the stress state in the outlet guide vanes can be schematically characterized as an oblique bend of a cantilever rod with clamps at both ends, one of which moves. With a decrease in the cross-section of rods (guide-vane profile) and a corresponding increase in their number, the stiffness of the rod system, on the one hand, increases by linear law (due to an increase in their number), and, on the other hand, it decreases by cubic law (due to decreasing cross-section). Thus, the maximum stresses in the rods (guide vanes) increase much faster. This conditional and fairly approximate interpretation explains the reason for the increase in SSS parameters with this approach to changing the axial dimensions of the diaphragm. It should also be noted the localization of high-stress areas in the outlet guide vanes.

Table 5. The maximum values of the SSS parameters of the second-stage diaphragm of the K-325-23.5 steam turbine HPC in the elastic state and during creep (100 thousand h), version 2 (k=1,24)

State	SSS parameter							
	Deflection W, mm		Radial stress σ_r, MPa				Circumstantial stress σ_θ, MPa	
	Seal	Blade root	Leading edge – body	Leading edge – rim	Trailing edge – body	Trailing edge – rim	Body	Rim
Elasticity	0.657	0.330	-222	355	266	178	78	-48
Creep	0.912	0.460	-155	210	154	97	54	-63

Table 6. The maximum values of the SSS parameters of the second-stage diaphragm of the K-325-23.5 steam turbine HPC in the elastic state and during creep (100 thousand hours), version 3 (k=1,48)

State	SSS parameter							
	Deflection W, mm		Radial stress σ_r, MPa				Circumstantial stress σ_θ, MPa	
	Seal	Blade root	Leading edge – body	Leading edge – rim	Trailing edge – body	Trailing edge – rim	Body	Rim
Elasticity	0.845	0.430	-315	453	335	217	98	-63
Creep	1.250	0.630	-213	277	201	126	75	-56

Table 7. The maximum values of the SSS parameters of the second-stage diaphragm of the K-325-23.5 steam turbine HPC in the elastic state and during creep (100 thousand h), version 4 (original guide vanes, diaphragm body and rim thicknesses are reduced)

State	SSS parameter							
	Deflection W, mm		Radial stress σ_r, MPa				Circumstantial stress σ_θ, MPa	
	Seal	Blade root	Leading edge – body	Leading edge – rim	Trailing edge – body	Trailing edge – rim	Body	Rim
Elasticity	0.839	0.420	-183	248	215	149	89	-54
Creep	1.150	0.570	-168	181	132	82	63	-57

In the second approach to reducing the diaphragm design size in the axial direction (version 4, original profile), rather considerable axial deflections are observed, which is explained by a decrease in the torsional stiffness of the diaphragm rim, to a greater extent, and of the body, to a lesser extent. The maximum stresses have increased slightly, meeting, in the state of creep, the criterion of long-term strength.

When modeling the joint of the guide-vane assembly with the diaphragm rim and body, the stiffness of the guide-vane shroud bands was taken into account, and the guide-vane profile discretization in thickness was two finite elements.

Conclusions and Proposals

Exploratory researches on more compact diaphragm designs (having reduced axial dimensions and satisfying the requirements for short- and long-term strength indicators) for the K-325-23.5 steam turbine HPC were conducted. The research was performed by calculation, and was based on a proven methodological basis using automated software.

Two approaches to determining promising diaphragm design versions were involved. The calculations showed that the approach that uses a proportional reduction of guide vane profiles with a simultaneous increase in the number of the guide vanes, and allows reducing the axial diaphragm dimensions, is not acceptable. During the implementation of this approach, the maximum values of axial deflections and stresses in the guide blades increase rapidly with increasing reduction coefficient of the guide-vane profile. In this case, the conditions of short- and long-term strengths are not met, starting with the value of the reduction coefficient of the profile k=1.24.

The approach according to which the guide-vane profile remains as in the original design, and the axial sizes of the diaphragm rim and body are reduced (reduction by 3.5 cm at an original diaphragm thickness value of 14 cm) has turned out to be more acceptable. The main thing in SSS assessments is rather limited maximum stresses in the outlet guide vane, satisfying the long-term strength criterion, and according to the short-term stress strength criterion, slightly exceeding the allowable values.

Thus, the proposed design version of the second-stage HPC diaphragm with reduced rim and body sizes while maintaining the original guide-vane profile can be considered to be promising.

It is known, and it should be emphasized, that the main problem in terms of strength are the outlet guide vanes of the assembly, which protrude beyond the diaphragm joint face. Totally understandable is the proposal to use, in the outlet guide vanes, a material with high heat resistance indicators, in particular, the limits of long-term strength. An example of the material used in power engineering is the 15H12VNMF (EI-802) steel, which has high mechanical properties at a temperature of 500 ºC: the yield strength σ_{ys}=440 MPa, the long-term strength at 100 thousand operating hours σ_{10}^{5}=244 MPa.

To reduce the axial deflections that are accumulated during creep, it is also possible to recommend replacing the diaphragm rim and body material with a material that is more resistant to creep, namely, the guide-vane material (15H11MF steel). A known design measure to reduce deflections during creep can be to replace the diaphragm rim joint to the HPC body, which limits the rotation of the rim under load, i.e. instead of free support, clamping is implemented. In addition to these measures, there can be others that will contribute to the main purpose of the work – to reduce axial diaphragm dimensions.

References

1. Shubenko-Shubin, L. A. (Eds.). (1973). *Prochnost parovykh turbin* [Strength of steam turbines]. Moscow: Mashinostroyeniye, 456 p. (in Russian).
2. Taylor, V. L. (1951). Stress and deflection tests of steam-turbine diaphragm. *Transactions of the ASME*. No. 7. P. 877–890.
3. Naumov, V. K. (1960). *Raschet diafragm parovykh i gazovykh turbin* [Calculation of diaphragms of steam and gas turbines]. In book: *Issledovaniya elementov parovykh i gazovykh turbin i osevykh kompressorov* [Research of elements of steam and gas turbines and axial compressors]. Leningrad: Mashgiz, pp. 310–312.
4. Sentsov, N. D. (1958). *O nekotorykh rezultatakh issledovaniya progibov i napryazheniy v svarnykh diafragmakh parovykh turbin* [About some results of research of deflections and stresses in welded diaphragms of steam turbines]. *Energomashinostroyeniye – Power Engineering*, no. 8, pp. 6–11 (in Russian).
5. Ingultsov, V. L. (1961). *Raschet diafragmy kak polukoltsa na uprugom opornom konture* [Calculation of a diaphragm as a half-ring on an elastic support contour]. *Energomashinostroyeniye – Power Engineering*, no. 11, pp. 1–5 (in Russian).
6. Kulagina, G. F. (1960). *Eksperimentalnoye issledovaniye napryazheniy i progibov diafragm* [Experimental study of stresses and deflections of diaphragms]. In book: *Issledovaniye ele-mentov parovykh i gazovykh turbin i osevykh kompressorov* [Research of elements of steam and gas turbines and axial compressors]. Leningrad: Mashgiz, pp. 333–346 (in Russian).
7. Zaytsev, B. F., Shulzhenko, N. G., & Asayenok, A. V. (2006). *Napryazhenno-deformirovannoye sostoyaniye i kontaktnyye yavleniya v opiranii diafragmy parovoy turbiny* [Stress-strain state and contact phenomena in the support of a steam turbine diaphragm]. *Problemy mashinostroyeniya – Journal of Mechanical Engineering*, vol. 3, no. 3, pp. 35–45 (in Russian).
8. Rozenblyum, V. I. (1954). *Raschet polzuchesti turbinnykh diafragm stupeney vysokogo davleniya* [Calculation of creep of turbine diaphragms of high pressure stages]. *Inzhenernyy sbornik – Engineering Collection*, vol. 20, pp. 49–54 (in Russian).
9. Tseytlin, I. Z. (1974). Raschet polzuchesti diafragm parovykh turbin [Calculation of creep of diaphragms of steam turbines]. *Energomashinostroyeniye – Power Engineering*, no. 12, pp. 6–11 (in Russian).
10. Vinogradov, N. N. (1970). *Issledovaniye polzuchesti naturnykh diafragm moshchnykh parovykh turbin* [Study of creep of full-scale diaphragms of powerful steam turbines]. *Teplovyye napryazheniya v elementakh konstruktsiy – Thermal stresses in structural elements*, iss. 10, pp. 35–43 (in Russian).
11. Malinin, N. N. (1975). *Prikladnaya teoriya plastichnosti i polzuchesti* [Applied theory of plasticity and creep]. Moscow: Mashinostroyeniye, 400 p. (in Russian).
12. (1986). *Turbiny parovyye statsionarnyye. Normy rascheta na prochnost korpusov tsilindrov i klapanov* [Stationary steam turbines. Standards for calculating the strength of cylinder and valve bodies]: OST 108.020.132-85. Moscow: Ministry of Power Engineering, 31 p. (in Russian).
13. Shul'zhenko, N. G., Zaitsev, B. F., Asaenok, A. V., Grishin, N. N., & Gubskii, A. N. (2016). Creep of steam-turbine diaphragm under variable loading conditions. *Strength of Materials*, vol. 48, iss. 6, pp. 733–739. https://doi.org/10.1007/s11223-017-9819-y.
14. Shabrov, N. N. & Znamenskaya, M. V. (1991). *Raschet diafragmy parovoy turbiny metodom superelementov* [Calculation of the steam turbine diaphragm by the superelement method]. *Trudy Tsentralnogo kotloturbinnogo instituta – Proceedings of the Central Boiler and Turbine Institute*, no. 265, pp. 43–47 (in Russian).

15. Shulzhenko, N. G., Asaenok, A. V., Zaitsev, B. F., Grishin, N. N., & Gubskii, A. N. (2012). Creep analysis of steam turbine welded diaphragm. *Strength of Materials*, vol. 44, iss. 4, pp. 419–428. https://doi.org/10.1007/s11223-012-9396-z.
16. Shakhmatov, M. V. & Shakhmatov, D. M. (2009). *Prochnost mekhanicheski neodnorodnykh svarnykh soyedineniy* [Strength of mechanically inhomogeneous welded joints]. Chelyabinsk: TSPS Svarka i kontrol Ltd, 223 p. (in Russian).
17. Vinokurov, V. A., Kurkin, S. A., & Nikolayev, G. A. (1996). *Svarnyye konstruktsii. Mekhanika razrusheniya i kriterii rabotosposobnosti* [Welded constructions. Fracture mechanics and performance criteria]. Moscow: Mashinostroyeniye, 576 p. (in Russian).
18. (1987). *Diafragmy parovykh statsionarnykh turbin. Raschety na prochnost* [Diaphragms of stationary steam turbines. Strength calculations]: OST 108.210.01-86. Moscow: Ministry of Power Engineering, NPO Central Boiler and Turbine Institute, 39 p. (in Russian).

Received 22 March 2021

Дослідження термоміцності діафрагм парової турбіни при зменшенні осьових габаритів

[1] Б. П. Зайцев, [2] В. Л. Швецов, [2] О. М. Губський, [2] С. А. Пальков, [1] Т. В. Протасова

[1] Інститут проблем машинобудування ім. А. М. Підгорного НАН України,
61046, Україна, м. Харків, вул. Пожарського, 2/10

[2] Акціонерне товариство «Турбоатом», 61037, Україна, м. Харків, пр. Московський, 199

Постановка задачі зменшення осьових габаритів діафрагм парових турбін пов'язана з проблемою їхньої модернізації, що виконується шляхом збільшення кількості ступенів з реактивним облопаченням та використанням існуючих фундаментів. Оцінку придатності варіантів конструкцій діафрагм з встановленими характеристиками потоку пари проведено з обмеженнями на виконання умов короткочасної та довготривалої міцності, а також накопичення осьових прогинів внаслідок повзучості. Для розрахункових досліджень запроваджено методологію, що використовує метод скінченних елементів та деформаційну теорію повзучості старіння Ю. М. Работнова. Розрахунок повзучості зведено до розв'язання пружно-пластичної задачі з діаграмою деформування, яку подано ізохронною кривою повзучості для вибраного часу. Використано програмне забезпечення, де передбачено автоматизацію побудови вихідної комп'ютерної моделі діафрагми з залученням креслень профілю напрямних лопаток, осьових перерізів тіла і обода та декількох геометричних параметрів. Розрахункова модель зварної діафрагми відтворює основні суттєві особливості її конструкції, властивостей матеріалів її елементів та навантаження парою. Пошукові дослідження діафрагм зі зменшеними осьовими розмірами проведено на прикладі діафрагм 2-го та 3-го ступенів циліндра високого тиску парової турбіни К-325-23,5. Вихідні конструкції 2-го та 3-го ступенів розглянуто як базові, по відношенню до яких за параметрами міцності і жорсткості співставлялись конструкції діафрагм, які вважалися за альтернативні. Отримано розрахункові дані для базових варіантів конструкції діафрагм для часу експлуатації 100 тисяч годин. Згідно з розрахунками максимальні прогини досягаються на краях діафрагми, а напруження, що є максимальними в місцях кріплення лопаток до обода і тіла, зазнають значного перерозподілу через повзучість. Задіяно різні підходи до зменшення осьових габаритів конструкції діафрагми 2-го ступеня циліндра високого тиску. При першому підході зменшення габаритів досягнуто пропорційним зменшенням профілю напрямних лопаток з відповідним збільшенням їх кількості. При другому – профіль залишився незмінним, але зменшено осьові розміри тіла і обода діафрагми. Досліджено параметри міцності в пружному стані на початку експлуатації і в умовах повзучості, а також накопичення осьових прогинів. На підставі порівнянь з базовою конструкцією встановлено, що більш дієвим є другий підхід. Наведено додаткові рекомендації щодо використання більш жароміцних сталей в крайніх напрямних лопатках та умов кріплення діафрагм в корпусі турбіни.

***Ключові слова**: парова турбіна, діафрагма, осьові габарити, повзучість, осьовий прогин, короткочасна і довготривала міцність.*

Література

1. Прочность паровых турбин / под ред. Л. А. Шубенко-Шубина. М.: Машиностроение, 1973. 456 с.
2. Taylor V. L. Stress and deflection tests of steam-turbine diaphragm. *Trans. ASME*. 1951. No. 7. P. 877–890.
3. Наумов В. К. Расчет диафрагм паровых и газовых турбин. *Исследования элементов паровых и газовых турбин и осевых компрессоров*. Л.: Машгиз, 1960. С. 310–312.

4. Сенцов Н. Д. О некоторых результатах исследования прогибов и напряжений в сварных диафрагмах паровых турбин. *Энергомашиностроение*. 1958. № 8. С. 6–11.
5. Ингульцов В. Л. Расчет диафрагмы как полукольца на упругом опорном контуре. *Энергомашиностроение*. 1961. № 11. С. 1–5.
6. Кулагина Г. Ф. Экспериментальное исследование напряжений и прогибов диафрагм. *Исследование элементов паровых и газовых турбин и осевых компрессоров*. Л.: Машгиз, 1960. С. 333–346.
7. Зайцев Б. Ф., Шульженко Н. Г., Асаенок А. В. Напряженно-деформированное состояние и контактные явления в опирании диафрагмы паровой турбины. *Пробл. машиностроения*. 2006. Т. 3. № 3. С. 35–45.
8. Розенблюм В. И. Расчет ползучести турбинных диафрагм ступеней высокого давления. *Инж. сб*. 1954. Т. 20. С. 49–54.
9. Цейтлин И. З. Расчет ползучести диафрагм паровых турбин. *Энергомашиностроение*. 1974. № 12. С. 6–11.
10. Виноградов Н. Н. Исследование ползучести натурных диафрагм мощных паровых турбин. *Тепловые напряжения в элементах конструкций*. 1970. Вып. 10. С. 35–43.
11. Малинин Н. Н. Прикладная теория пластичности и ползучести. М.: Машиностроение, 1975. 400 с.
12. Турбины паровые стационарные. Нормы расчета на прочность корпусов цилиндров и клапанов: ОСТ 108.020.132-85. М.: Мин-во энерг. машиностроения, 1986. 31 с.
13. Shul'zhenko N. G., Zaitsev B. F., Asaenok A. V., Grishin N. N., Gubskii A. N. Creep of steam-turbine diaphragm under variable loading conditions. *Strength Materials*. 2016. Vol. 48. Iss. 6. P. 733–739. https://doi.org/10.1007/s11223-017-9819-y.
14. Шабров Н. Н., Знаменская М. В. Расчет диафрагмы паровой турбины методом суперэлементов. *Тр. Центр. котлотурбин. ин-та.* 1991. № 265. С. 43–47.
15. Shulzhenko N. G., Asaenok A. V., Zaitsev B. F., Grishin N. N., Gubskii A. N. Creep analysis of steam turbine welded diaphragm. *Strength Materials*. 2012. Vol. 44. Iss. 4. P. 419–428. https://doi.org/10.1007/s11223-012-9396-z.
16. Шахматов М. В., Шахматов Д. М. Прочность механически неоднородных сварных соединений. Челябинск: ООО «ЦПС Сварка и контроль», 2009. 223 с.
17. Винокуров В. А., Куркин С. А., Николаев Г. А. Сварные конструкции. Механика разрушения и критерии работоспособности. М.: Машиностроение, 1996. 576 с.
18. Диафрагмы паровых стационарных турбин. Расчеты на прочность. ОСТ 108.210.01-86. М.: Мин-во энерг. машиностроения, НПО Центр. котлотурбин. ин-т, 1987. 39 с.